

# Evidence of new finite beam plasma instability for magnetic field generation

Amita Das<sup>1,\*</sup>, Atul Kumar<sup>1</sup>, Chandrasekhar Shukla<sup>1</sup>, Ratan Kumar Bera<sup>1</sup>, Deepa Verma<sup>1</sup>, Bhavesh Patel<sup>2</sup>, Y. Hayashi<sup>3</sup>, K. A. Tanaka<sup>4</sup>, Amit D. Lad<sup>5</sup>, G. R. Kumar<sup>5</sup>, and Predhiman Kaw<sup>1</sup>

<sup>1</sup>*Institute for Plasma Research, HBNI, Bhat, Gandhinagar - 382428, India*

<sup>2</sup>*Institute for Plasma Research, Bhat, Gandhinagar - 382428, India*

<sup>3</sup>*Graduate School of Engineering, Osaka University, Suita, Osaka 565-0871 Japan*

<sup>4</sup>*Extreme Laser Infrastructure-Nuclear Physics 30 Reactorului,  
PO Box MG-6, Bucharest Magurele 077125 Romania and*

<sup>5</sup>*Tata Institute of Fundamental Research, 1 Homi Bhabha Road, Mumbai 400005, India*

**We demonstrate by computer simulations, laser plasma experiments and analytic theory that a hitherto unknown instability is excited in the beam plasma system with finite transverse size. This instability is responsible for the generation of magnetic fields at scales comparable to the transverse beam dimension which can be much longer than the electron skin depth scale. This counterintuitive result arises due to radiative leakage associated with finite beam boundaries which are absent in conventional infinite periodic systems considered in earlier simulations as well as theoretical analyses and may trigger a reexamination of hitherto prevalent idea.**

The dynamical evolution of intense magnetic fields and associated current pulses plays an important role in a variety of plasma physics problems. These include plasma switches, designing of novel radiation and charged particle sources, laser driven fusion and also laboratory simulation of astrophysical phenomena etc [1–6]. The current pulses may be generated and driven into a solid target by an intense, femtosecond laser that generates a hot, dense plasma at the surface. It is now well known that giant current pulses produced in such an interaction induce return currents from the thermal plasma electrons and these two types of currents are subject to electromagnetic instabilities. It is widely believed that the well known Weibel instability [7, 8] separates these initially superimposed counter currents and leads to giant magnetic field generation in intense laser driven plasmas. Countless analytical and simulation studies have explored this instability and predicted that the scale at which the magnetic field gets generated characterizes this instability and is essentially the (local) skin depth of the plasma. The nonlinear inverse cascade mechanism is invoked for subsequent long scale generation of magnetic fields. This belief had strong support from all plasma simulations which demonstrated unambiguously that the scale at which the energy is driven into the magnetic field is at the skin depth scale. In this manuscript we provide convincing evidence that this is not the correct physical situation but is merely an artifact of boundless beam plasma interaction in simulations as well as theoretical analyses. We demonstrate through laser plasma experiments and finite beam size simulations using different variety of codes, that the energy is input preferentially into the plasma at the scale size of the beam (in the case of laser experiments this is at the spot size of the irradiating laser). We show that magnetic field generation caused by the electron currents first occurs at the scale size of the boundary and only much later does the Weibel instability

kick in at the skin depth scale. This is a new instability mechanism of magnetic field generation that may tentatively be called 'finite beam instability' (FBI). It has been demonstrated with the help of a detailed linearized perturbation analysis that the characteristic features of FBI are in marked contrast with Weibel instability. Such a behaviour finds support in our finite beam size simulations. We show that the FBI dominates the Weibel instability at the initial stage and has its origin in the effect of radiative loss from negative energy waves in a manner analogous to the radiative instability of a leaky waveguide [9, 10]. We believe our study is an important step in establishing the crucial role that finite size effects can play in qualitatively changing the physical nature of eigen modes in beam plasma system.

The choice of infinite beam - plasma periodic system considered in earlier studies [11] is based on an inherent assumption that the boundary effects due to the finite system would merely have a small incremental impact. This assumption, however, turns out to be incorrect. We show with PIC as well as two-fluid simulations that when a beam with finite transverse extent is considered, an entirely new instability associated with the finite size of the beam appears which generates magnetic fields at the scale of the beam size right from the very beginning. Secondly, the sheared electron flow configuration at the two edges of the finite beam is seen to be susceptible to Kelvin Helmholtz instability [12, 13]. Weibel appears only in the bulk region of the beam at a later stage. Thus, there are three sources of magnetic fluctuations in a finite beam system - the new Finite Beam Instability (FBI) and KH instability operating at the edge and the usual Weibel destabilization process occurring in the bulk region. The theoretical description of the FBI has been provided here which is followed up by evidences from simulations (both PIC and fluid [LCPFCT[14]]) and experimental data[4] where the appearance of magnetic field at the laser spot

size (much larger than the skin depth) at very early stage can only be accounted via this instability. The conventional Weibel destabilization route of the beam plasma system can never account for such an effect.

An equilibrium configuration of the beam plasma system in 2-D  $x - y$  plane is considered as shown in Fig.1. The central region II from  $-a \leq y \leq a$  carries the beam current and an oppositely flowing background plasma current, which balances each other. In region I and region III the plasma is static and at rest. The charge neutralization in equilibrium is achieved by balancing the total electron density by the background ion density, viz.,  $\sum_{\alpha} n_{0\alpha} = n_{0i}$  in all the three regions. The electron flow velocity in region I and III is zero, whereas in region II it satisfies the condition of zero current, i.e.  $\sum_{\alpha} n_{0\alpha} v_{0\alpha x} = 0$ . Here the suffix  $\alpha$  stands for  $b$  and  $p$  representing the beam and plasma electrons. The linearized perturbation of this equilibrium is considered with variations in  $y$  and  $t$  only. The flow is confined in  $x - y$  plane, so we have  $B_{1z}$ ,  $E_{1x}$  and  $E_{1y}$  (where the suffix  $x, y$ , and  $z$  denotes the components and B and E represents the magnetic and electric fields) only as the perturbed dominant fields. Eliminating all the perturbed fields in terms of  $E_{1x}$  leads to the following differential equation:

$$[f_2 E'_{1x}]' - g_2 E_{1x} = 0 \quad (1)$$

Here

$$f_2 = 1 + \frac{S_4}{\omega^2} - \frac{S_3^2}{\omega^2(S_1 - \omega^2)} \quad (2)$$

$$g_2 = S_2 - \omega^2 \quad (3)$$

where

$$S_1 = \sum_{\alpha} \frac{n_{0\alpha}}{n_0 \gamma_{0\alpha}}; \quad (4)$$

$$S_2 = \sum_{\alpha} \frac{n_{0\alpha}}{n_0 \gamma_{0\alpha}^3}; \quad (5)$$

$$S_3 = \sum_{\alpha} \frac{n_{0\alpha} v_{0x\alpha}}{n_0 \gamma_{0\alpha}}; \quad (6)$$

$$S_4 = \sum_{\alpha} \frac{n_{0\alpha} v_{0x\alpha}^2}{n_0 \gamma_{0\alpha}}; \quad (7)$$

It should be noted that  $S_3$  and  $S_4$  are finite only when there is an equilibrium flow in the two fluid electron depiction. Furthermore, if the flow velocities of the two electron species are equal and opposite then  $S_3 = 0$ .

The homogeneous limit of Califano *et. al.*[15] can be easily recovered if we take Fourier transform of Eq.(1). The homogenous equation yields the dispersion relation for the Weibel growth rate. We now seek the possibilities for obtaining purely growing modes in a finite system. For this purpose we multiply Eq.(1) by  $E_{1x}$ , replace  $\omega^2 = -\gamma^2$  (for purely growing modes) and integrate over  $y$  over region II, i.e. from  $-a$  to  $a$ . This yields:

$$\int_{-a}^a [E_{1x}(f_2 E'_{1x})' - g_2 E_{1x}^2] dy = 0 \quad (8)$$

Upon integrating by parts we obtain

$$f_2 [E_{1x} E'_{1x}]|_{-a}^a - \int_{-a}^a \left\{ f_2 [E'_{1x}]^2 + g_2 E_{1x}^2 \right\} dy = 0 \quad (9)$$

In region II,  $f_2$  and  $g_2$  being constant, we can take them outside the integral. Thus Eq.(9) can be written as

$$f_2 [E_{1x} E'_{1x}]|_{-a}^a - f_2 \int_{-a}^a [E'_{1x}]^2 dy - g_2 \int_{-a}^a E_{1x}^2 dy = 0 \quad (10)$$

If the boundary term is absent, as in the case of infinite homogeneous system, then Eq.(10) can be satisfied for a finite value of  $E_{1x}$ , provided second and third terms have opposite signs. The integrand being positive definite this is possible provided  $g_2$  and  $f_2$  have opposite signs. The definitions of  $g_2$  and  $f_2$  in terms of  $\gamma^2$  are

$$f_2 = 1 + \frac{S_3^2}{\gamma^2(S_1 + \gamma^2)} - \frac{S_4}{\gamma^2}$$

$$g_2 = S_2 + \gamma^2$$

Since  $g_2$  is positive, the only possible way for  $f_2$  to be negative is to have  $S_4/\gamma^2$  dominate over the first two terms of  $f_2$ . Thus, the conventional Weibel gets driven by  $S_4$ . It is also obvious that  $S_3$  provides a stabilizing contribution making it more difficult for  $f_2$  to become negative. A finite value of  $S_3$  implies a non-symmetric flow configuration, i.e. one for which the two electron species have different flow speeds.

For finite system, something interesting happens when boundary contribution are retained. The value of  $[E_{1x} E'_{1x}]|_{-a}^a$  should be positive as  $E_{1x}^2$  should increase as one enters region II from region I (at  $y = -a$ ) and it should decrease at  $y = a$ . Thus the sign of first term will be determined by the sign of  $f_2$ . Another way to understand the positivity of the sign of  $[E_{1x} E'_{1x}]|_{-a}^a$  is by realizing that this term is essentially the radiative flux moving outside region II which can only be positive. This is seen by casting it in the form of the Poynting flux by expressing the derivative of  $E_{1x}$  in terms of  $B_{1z}$ .

There exists the possibility then that the first term of Eq.(10) has a finite contribution to balance the second and the third terms. Thus even if  $f_2$  and  $g_2$  have same signs (positive) Eq.(10) can be satisfied for a finite  $E_{1x}$  if the boundary is finite and boundary terms contribute through the Poynting flux. It should be noted that the instability driven in this case is different from the Weibel mode as the boundary terms are responsible for it and  $S_3$  is playing an altogether different role of destabilization. Furthermore, it is interesting to observe that Equation(10) can be satisfied most easily by the boundary contribution provided the variations in  $E_{1x}$  in the bulk is minimal so as to have minimal (close to zero) contribution from the second term. Thus the instability

driven by the boundary term would have a preference for long scale excitation.

PIC simulations using OSIRIS [16, 17], PICPSI [18] and EPOCH [19] were carried out for the case of a forward beam current and a compensating return plasma current of a finite transverse extent at  $t = 0$  shown as the equilibrium configuration in Fig.(1). The simulations were carried out in both 2-D and 3-D. In 3-D compensating cylindrical beam currents of diameter  $2a$  was chosen. The 2-D simulations were carried for a box size of  $25c/\omega_{pe} \times 25c/\omega_{pe}$ . The beam was chosen to be confined within an extent of  $2a = 5c/\omega_{pe}$ . Various choices of beam and background electron density have been chosen. In Fig.2 we have chosen to show the results (evolution of magnetic field as well as density) for beam electron density of  $0.1n_0$  moving along  $\hat{x}$  with a velocity of  $0.9c$  in a central region( from  $y = 10c/\omega_{pe}$  to  $y = 15c/\omega_{pe}$  ) i.e., with a transverse extent of  $5c/\omega_{pe}$ . In the same region, a shielding return current along  $-\hat{x}$  of background electrons with density  $0.9n_0$  has been taken to flow with a velocity of  $0.1c$ . Here,  $n_0$  is the density of background ions which are at rest everywhere. In the remaining region from  $y = 0$  to  $10c/\omega_{pe}$  and  $15$  to  $20 c/\omega_{pe}$  electrons and ions both with density  $n_0$  are at rest. Thus, the plasma everywhere is neutral with electron density balancing the density of background plasma ions. In the central beam region, the beam current is exactly compensated by the return shielding current. The movie uploaded as supplementary material shows the generation and evolution magnetic field for this particular configuration. Snapshots of the evolution at various times have been depicted in Fig. 2 in the form of 2-D color plots for the  $z$  component of the magnetic field and the perturbed charge density respectively.

From these plots, it is clearly evident that there are three distinct phases of evolution. During the first phase from  $t = 0.12\omega_{pe}^{-1}$  to  $t = 30\omega_{pe}^{-1}$  perturbed  $z$  component of magnetic field along  $\hat{z}$  (transverse to both flow and inhomogeneity) appear at the edges with opposite polarity. This magnetic field has no  $x$  dependence and is a function of  $y$  alone. The magnetic field perturbations are seen to grow with time and also expand in  $y$  from the edges in both the directions at the speed of light. The electron density perturbations, which also appear at the edge, on the other hand, remain confined at the edge during this phase. This first phase of the evolution thus can be characterized by the appearance of magnetic field perturbations with variations only along  $\hat{y}$ , the transverse direction. This fits the analytical description very well. Keeping in view that the structures do not seem to vary with respect to the  $x$ , the 1-D profiles along  $y$  have been shown in Fig. 3 for  $E_{1x}$ . As predicted for the FB mode theoretically,  $E_{1x}$  shows minimal variation inside the beam region. The PIC simulations were also repeated for the case where  $S_3 = 0$  was taken by a choice of symmetric flow. In this case we observed that the FB mode

did not appear. This shows that  $S_3$  plays a destabilizing role for this instability, just the opposite role it has for the Weibel mode. During the second phase from  $t = 30\omega_{pe}^{-1}$  the Kelvin Helmholtz (KH) like perturbations appear at the edge of the current. Around this time one can also observe appearance of faint Weibel perturbations in the bulk central region. Both the KH and the Weibel mode have variations along both  $\hat{y}$  and  $\hat{x}$  directions.

We also provide the snap shot from 3-D simulations in Fig. (4) for a finite beam propagating in the plasma at a very late time  $t = 78.6\omega_{pe}^{-1}$  in which both FBI and the Weibel mode can be observed. These observations with characteristics three phase developments have been repeatedly observed in both 2-D and 3-D from a variety of simulations carried out with different PIC as well as fluid codes.

A comparison of the evolution of the magnetic field spectra for the periodic infinite system as well as the finite beam case has been provided at various times in Fig. 5. It is clear from the figure that for the periodic infinite case the peak of spectral power appears at the electron skin depth scale initially. In this case, the spectral power only subsequently cascades towards longer scales via inverse cascade mechanism which is considerably slow. On the other hand, for the finite case, it can be clearly observed that the spectral peak appears at the beam size right from the very beginning.

In laboratory laser plasma experiments the electron beam width would be finite, typically commensurate with the dimension of the laser focal spot. It would, therefore, be interesting to look for evidences of finite beam instability in the laser plasma experiments. The experiments were carried out at the Tata Institute of Fundamental Research, Mumbai using a 20 TW Ti: Sapphire laser. The laser is capable of delivering 30 fs, 800 nm pulses at 10 Hz. A p-polarized pump laser with 120 mJ energy was focussed on an aluminium coated BK7 glass target with an  $f/3$  off-axis parabola. The resulting peak intensity was  $3 \times 10^{18} W/cm^2$ . A second harmonic (400nm) probe pulse was time delayed with respect to the pump pulse. The intensity of probe pulse was adjusted to be  $10^{11} W/cm^2$ . A second harmonic probe can penetrate up to four times the critical density corresponding 800nm pum radiation[20]. A magneto-optic Cotton-Mouton polarimetry set-up [4, 20] was utilized to spatially resolve ellipticity. The induced magnetic field is inferred from the ellipticity data [21]. The power spectra have been calculated as per Ref. [4] and shown to peak at the focal spot of the laser pulse right from the very beginning. In Fig. (6) observations at a time delay of 0.4 pico-seconds have been shown. It is clear from the figure that the longest observed scale of focal spot has the maximum power at such an early time. Thus, this experiment provides another evidence for the existence of the FBI instability.

While the KH and the Weibel modes are well known

and have been discussed extensively in the literature, the FBI has neither been observed nor been described anywhere. This qualitatively new result arises because the infinite periodic approximation is unable to consider effects due to radiative leakage at the boundaries. The implications of this particular instability on magnetic field generation need to be evaluated in different contexts. For instance, it is likely that the finite size jets emanating from astrophysical objects are susceptible to this particular instability. This work also suggests that the finite size considerations in many other systems need to be looked afresh to unravel new effects which might have been overlooked so far.

Finally, some general remarks. Homogeneity and infinite extent are idealizations that permeate all physical models as they simplify descriptions because of the resulting uniformity and reduced dimensionality of the problem. Real systems, however, are finite and deviations from idealization can lead to novel physical effects. This lesson has been learned from time to time. For instance, the existence of Casimir effect [22, 23] leading to attractive force between two plates due to vacuum fluctuations, einzel lense [24, 25] - which enables focussing of charged particles using fringing fields at capacitor edges, existence of surface plasmon modes [26] distinct from bulk modes, discrete eigen modes in waveguides etc., are some examples of finite size boundaries leading to new effects. The present manuscript demonstrates another outstanding example in this context.

### Acknowledgments

AD acknowledges the DAE-SRC-ORI grant Government of India. GRK acknowledges J C Bose Fellowship grant (JCB-037/2010) from the Department of Science and Technology, Government of India. A part of the research has also been supported by the S-level funding 15H05751, JSPS Japan.

---

\* Electronic address: amita@ipr.res.in

- [1] K. B. Wharton, S. P. Hatchett, S. C. Wilks, M. H. Key, J. D. Moody, V. Yanovsky, A. A. Offenberger, B. A. Hammel, M. D. Perry, and C. Joshi, "Experimental measurements of hot electrons generated by ultraintense laser-plasma interactions on solid-density targets," *Phys. Rev. Lett.*, vol. 81, pp. 822–825, Jul 1998.
- [2] K. A. Brueckner and S. Jorna, "Laser-driven fusion," *Rev. Mod. Phys.*, vol. 46, pp. 325–367, Apr 1974.
- [3] R. Betti and O. A. Hurricane, "Inertial-confinement fusion with lasers," *Nature Physics*, vol. 12, no. May, pp. 435–448, 2016.
- [4] S. Mondal, V. Narayanan, W. J. Ding, A. D. Lad, B. Hao, S. Ahmad, W. M. Wang, Z. M. Sheng, S. Sengupta, P. Kaw, A. Das, and G. R. Kumar, "Direct observation of turbulent magnetic fields in hot, dense laser produced plasmas," *Proceedings of the National Academy of Sciences*, vol. 109, no. 21, pp. 8011–8015, 2012.
- [5] A. B. Remington, A. David, P. R., Drake, and T. Hideaki, "Modeling astrophysical phenomena in the laboratory with intense lasers," *Science*, vol. 284, no. 5419, pp. 1488–1493, 1999.
- [6] G. Chatterjee, K. M. Schoeffler, P. Kumar Singh, A. Adak, A. D. Lad, S. Sengupta, P. Kaw, L. O. Silva, A. Das, and G. R. Kumar, "Magnetic turbulence in a table-top laser-plasma relevant to astrophysical scenarios," *Nature Communication*, vol. 8, 2017.
- [7] E. S. Weibel, "Spontaneously growing transverse waves in a plasma due to an anisotropic velocity distribution," *Phys. Rev. Lett.*, vol. 2, pp. 83–84, Feb 1959.
- [8] F. Pegoraro, S. V. Bulanov, F. Califano, and M. Lontano, "Nonlinear development of the weibel instability and magnetic field generation in collisionless plasmas," *Physica Scripta*, vol. T63, no. 3, pp. 262–265, 1996.
- [9] M. Miyagi, "Bending losses in hollow and dielectric tube leaky waveguides," *Appl. Opt.*, vol. 20, pp. 1221–1229, Apr 1981.
- [10] D. Botez, L. Mawst, P. Hayashida, G. Peterson, and T. J. Roth, "Highpower, diffractionlimitedbeam operation from phaselocked diodelaser arrays of closely spaced leaky waveguides (antiguides)," *Applied Physics Letters*, vol. 53, no. 6, pp. 464–466, 1988.
- [11] Y. Sentoku, K. Mima, Z. M. Sheng, P. Kaw, K. Nishihara, and K. Nishikawa, "Three-dimensional particle-in-cell simulations of energetic electron generation and transport with relativistic laser pulses in overdense plasmas," *Phys. Rev. E*, vol. 65, p. 046408, Mar 2002.
- [12] A. Das and P. Kaw, "Nonlocal sausage-like instability of current channels in electron magnetohydrodynamics," *Physics of Plasmas*, vol. 8, no. 10, pp. 4518–4523, 2001.
- [13] C. Shukla, A. Das, and K. Patel, "Particle-in-cell simulation of two-dimensional electron velocity shear driven instability in relativistic domain," *Physics of Plasmas*, vol. 23, no. 8, p. 082108, 2016.
- [14] J. Boris, A. Landsberg, E. Oran, and J. Gardner, "Lcpfct - a flux-corrected transport algorithm for solving generalized continuity equations.," *NRL/MR/6410-93-7192*, no. NRL Memorandum Report 93-7192., 1993.
- [15] F. Califano, R. Prandi, F. Pegoraro, and S. V. Bulanov, "Nonlinear filamentation instability driven by an inhomogeneous current in a collisionless plasma," *Phys. Rev. E*, vol. 58, pp. 7837–7845, Dec 1998.
- [16] R. A. Fonseca, L. O. Silva, F. S. Tsung, V. K. Decyk, W. Lu, C. Ren, W. B. Mori, S. Deng, S. Lee, T. Katsouleas, and J. C. Adam, *OSIRIS: A Three-Dimensional, Fully Relativistic Particle in Cell Code for Modeling Plasma Based Accelerators*, pp. 342–351. Berlin, Heidelberg: Springer Berlin Heidelberg, 2002.
- [17] R. A. Fonseca, S. F. Martins, L. O. Silva, J. W. Tonge, F. S. Tsung, and W. B. Mori, "One-to-one direct modeling of experiments and astrophysical scenarios: pushing the envelope on kinetic plasma simulations," *Plasma Physics and Controlled Fusion*, vol. 50, no. 12, p. 124034, 2008.
- [18] C. Shukla, A. Das, and K. Patel, "Effect of finite beam width on current separation in beam plasma system: Particle-in-Cell simulations," vol. arxiv:1508.07701[physics.plasm-ph], pp. 1–8, 2015.

- [19] T. D. Arber, K. Bennett, C. S. Brady, A. Lawrence-Douglas, M. G. Ramsay, N. J. Sircombe, P. Gillies, R. G. Evans, H. Schmitz, A. R. Bell, and C. P. Ridgers, “Contemporary particle-in-cell approach to laser-plasma modelling,” *Plasma Physics and Controlled Fusion*, vol. 57, no. 11, p. 113001, 2015.
- [20] G. Chatterjee, P. K. Singh, A. Adak, A. D. Lad, and G. R. Kumar, “High-resolution measurements of the spatial and temporal evolution of megagauss magnetic fields created in intense short-pulse laser-plasma interactions,” *Review of Scientific Instruments*, vol. 85, no. 1, p. 013505, 2014.
- [21] A. S. Sandhu, A. K. Dharmadhikari, P. P. Rajeev, G. R. Kumar, S. Sengupta, A. Das, and P. K. Kaw, “Laser-generated ultrashort multimegagauss magnetic pulses in plasmas,” *Phys. Rev. Lett.*, vol. 89, p. 225002, Nov 2002.
- [22] H. B. G. Casimir and D. Polder, “The influence of retardation on the london-van der waals forces,” *Phys. Rev.*, vol. 73, pp. 360–372, Feb 1948.
- [23] H. B. G. Casimir, “On the attraction between two perfectly conducting plates,” *Proc. K. Ned. Akad. Wet.*, vol. 51, pp. 793–795, 1948.
- [24] H. Liebl, *Applied Charged Particle Optics*. Springer-Verlag, Berlin, 2008.
- [25] R. Feynman, R. B. Leighton, and M. Sands, *The Feynman Lectures on Physics*, vol. 2. Addison-Wesley, Reading, Massachusetts, 1964.
- [26] E. A. Stern and R. A. Ferrell, “Surface plasma oscillations of a degenerate electron gas,” *Phys. Rev.*, vol. 120, pp. 130–136, Oct 1960.
- [27] J. Clyne, P. Mininni, A. Norton, and M. Rast, “Interactive desktop analysis of high resolution simulations: application to turbulent plume dynamics and current sheet formation,” *New Journal of Physics*, vol. 9, no. 8, p. 301, 2007.
- [28] J. Clyne and M. Rast, “A prototype discovery environment for analyzing and visualizing terascale turbulent fluid flow simulations,” in *Electronic Imaging 2005*, pp. 284–294, International Society for Optics and Photonics, 2005.

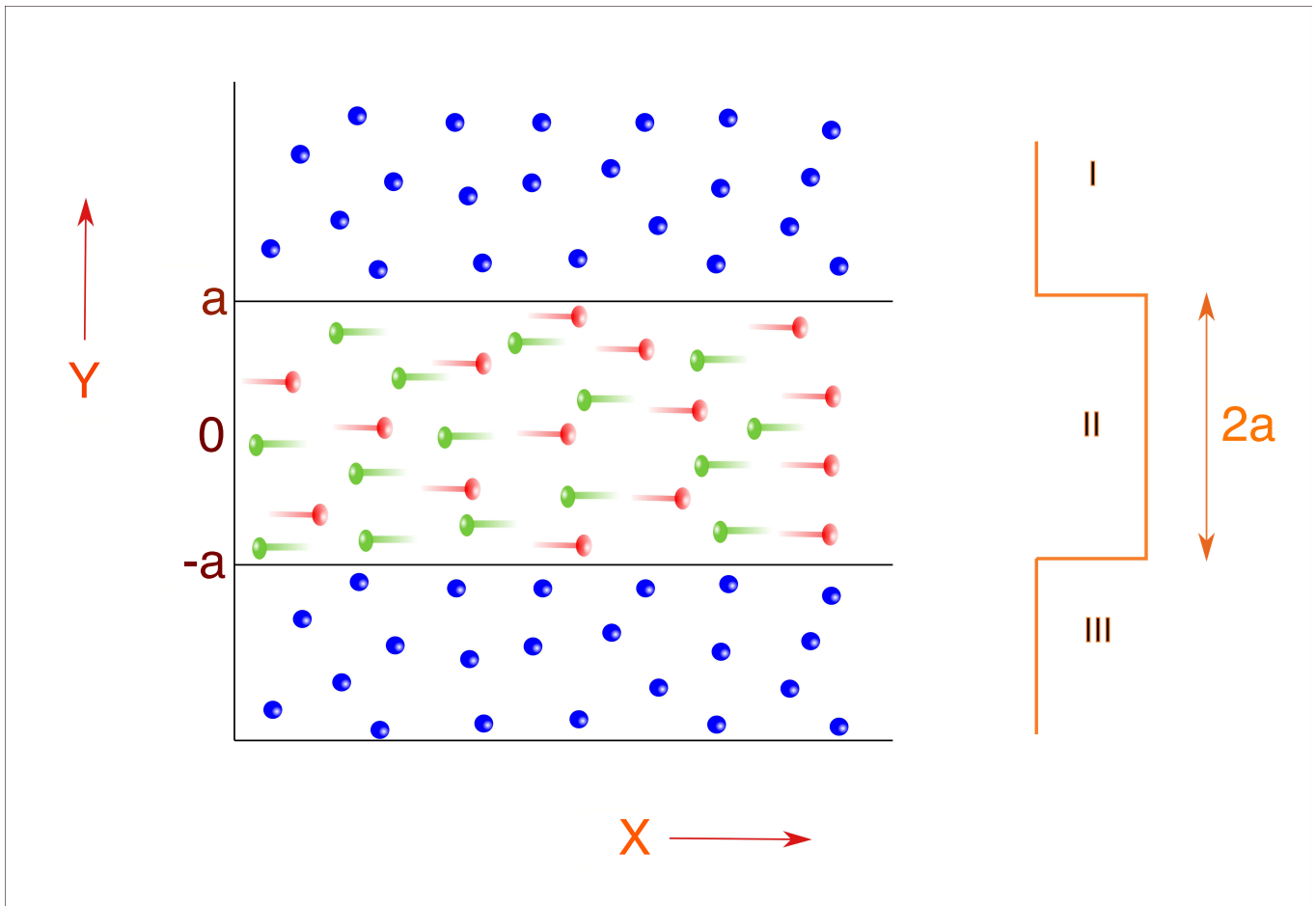


FIG. 1: Schematics of 2D-equilibrium geometry of the beam plasma system where beam has finite width ' $2a$ ' in the transverse direction

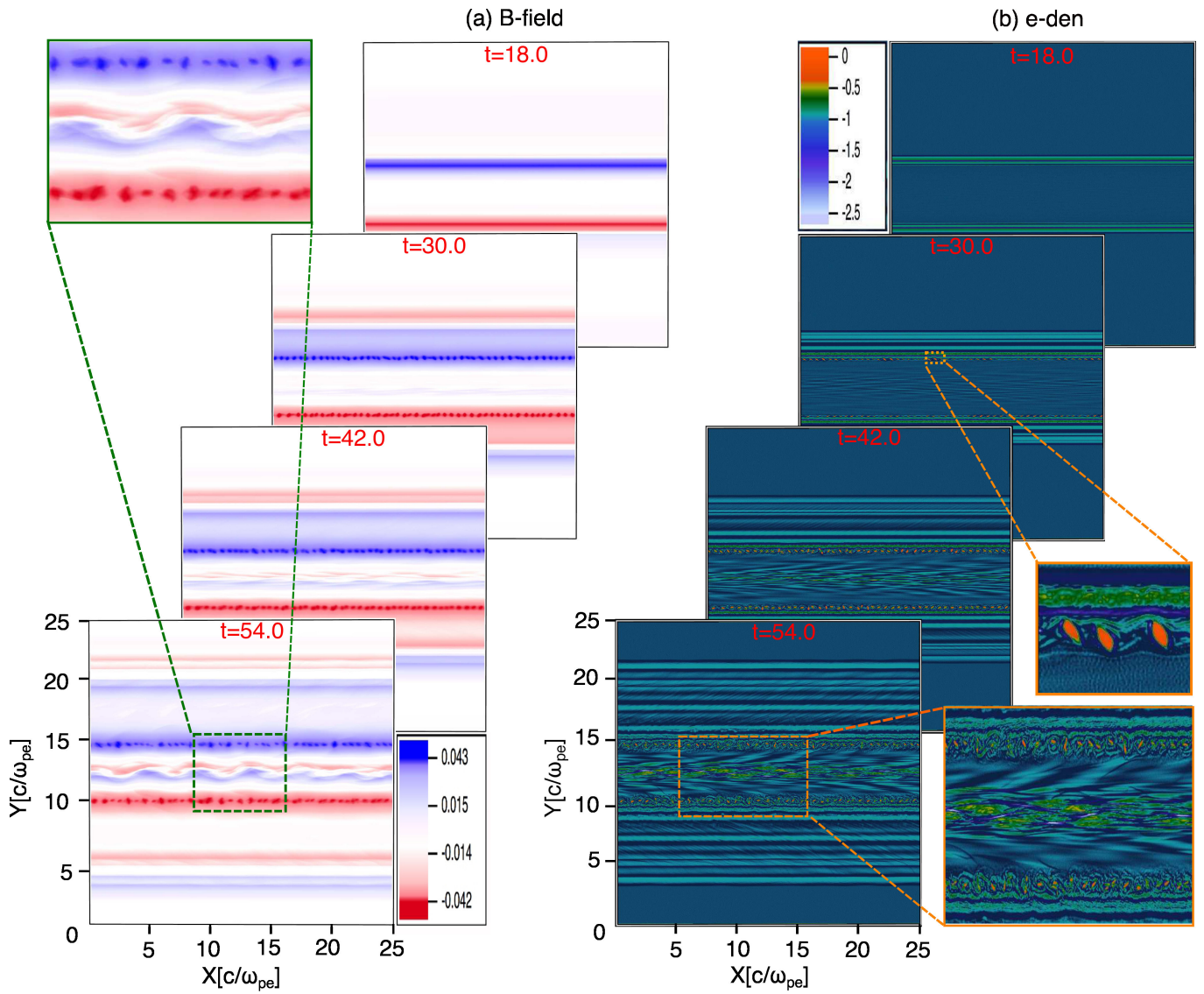


FIG. 2: Snapshots of magnetic field  $B$  [in the units of  $(mc\omega_{pe}/e)$ ] and electron density evolution in time  $t$  [in the unit of  $\omega_{pe}^{-1}$ ] has been depicted [prepared by Vapor [27, 28]]. Case(a) and Case(b) depicts the spatio temporal evolution of magnetic field  $B_z$  and the electron density respectively. At time  $t = 18.0$  only FBI development ( $B_z$  field with the opposite polarity) can be seen, at  $t = 30$  KH mode at the beam edge and a faint Weibel instability in the bulk appears. At  $t = 42.0$  and  $t = 54.0$  all the three instabilities can be observed clearly.

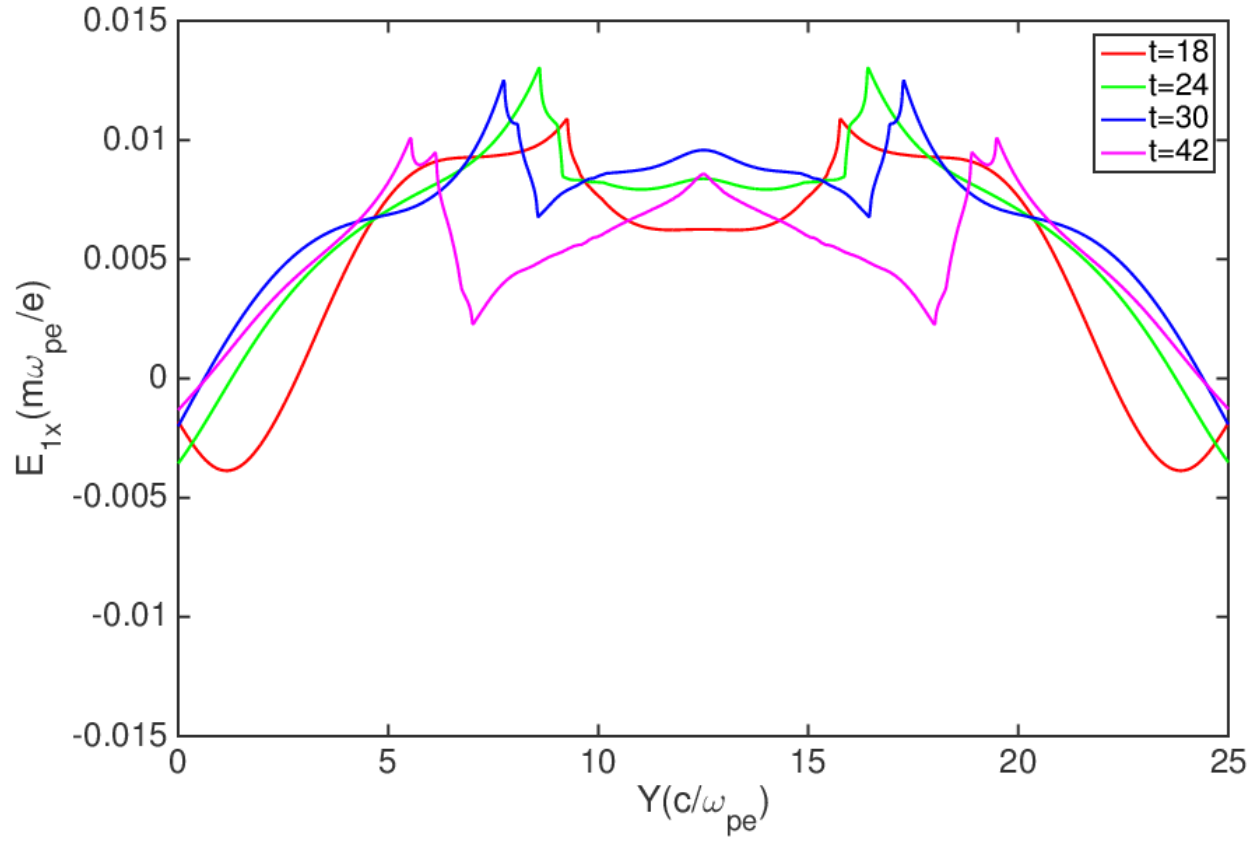


FIG. 3: Evolution of  $E_{1x}$  profile as a function of  $y$  showing the minimal variation inside the beam region in the beginning in conformity with FBI mode.



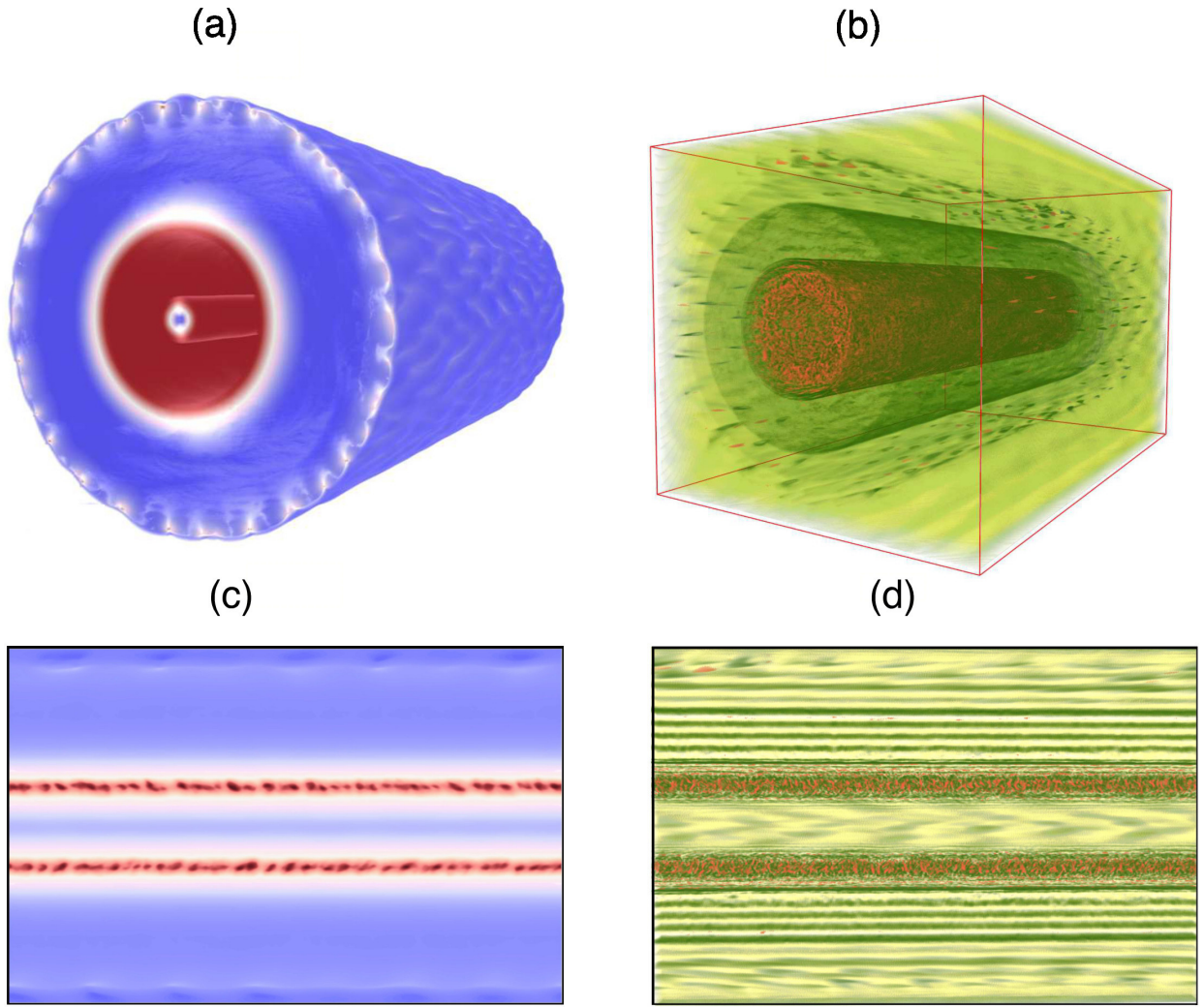


FIG. 4: Snapshots of 3D PIC simulation with OSIRIS [prepared by Vapor [27, 28]] at time  $t = 78.6$  in the unit of  $\omega_{pe}^{-1}$ . Subplots (a) and (b) depict 3D volume rendering of poloidal magnetic field and electron density respectively. In subplot (c) and (d) the cross sectional view in the  $r - z$  plane have been shown for the magnetic field and the electron density respectively. In these 3-D snapshots also all the three instabilities viz., FBI and KH at the edge of the beam and Weibel in the bulk region of the beam are clearly evident.

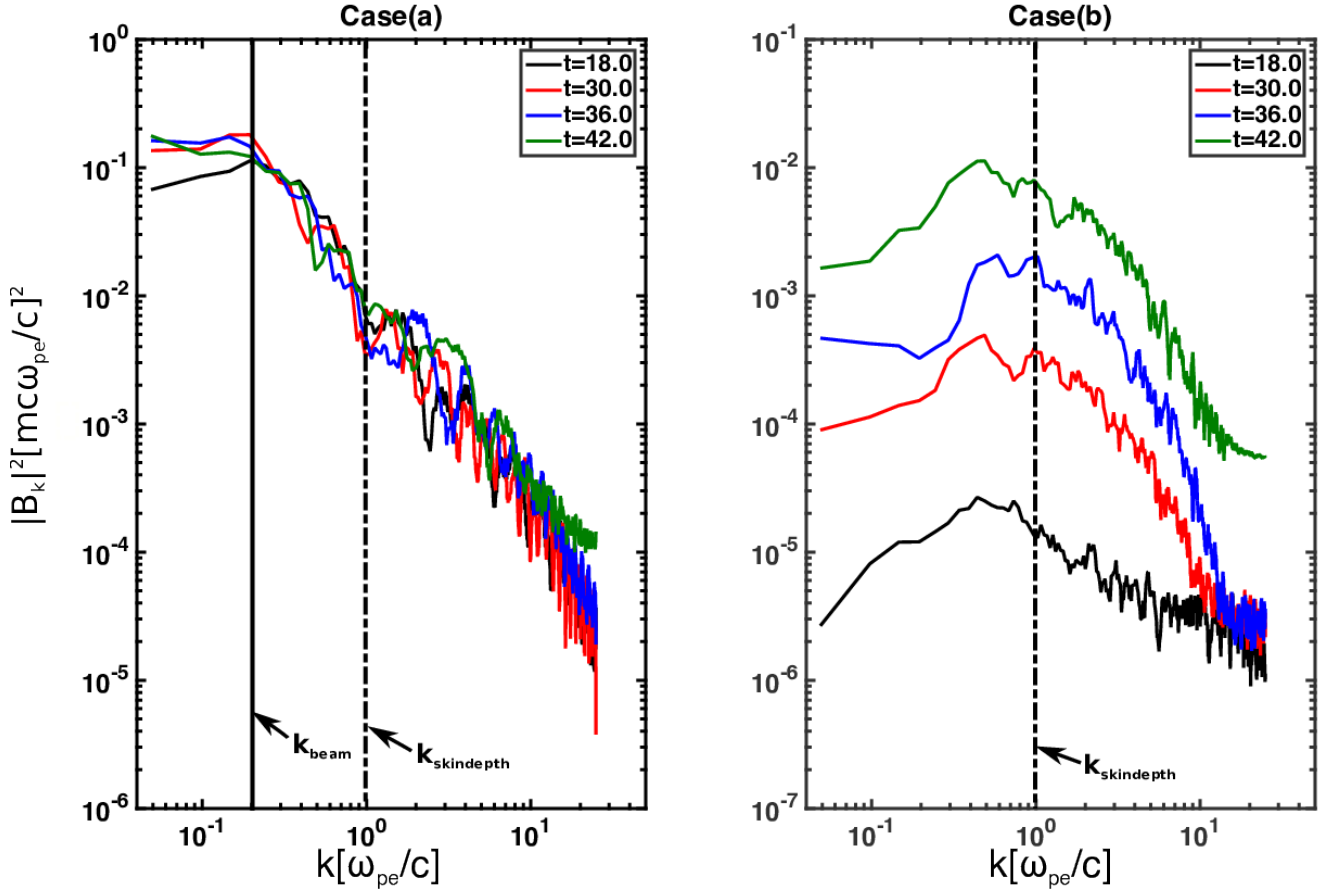


FIG. 5: Evolution of Magnetic field spectra from PIC simulations with OSIRIS Case(a) Finite beam-plasma system was considered in simulation. The spectral maximum is at at the width of the beam right from the beginning; Case(b)-Periodic box simulations corresponding to infinite beam-plasma system where peak of the field spectra appears at the electron skin depth due to Weibel mode and the nonlinear cascade towards long scale can be seen to be very slow.

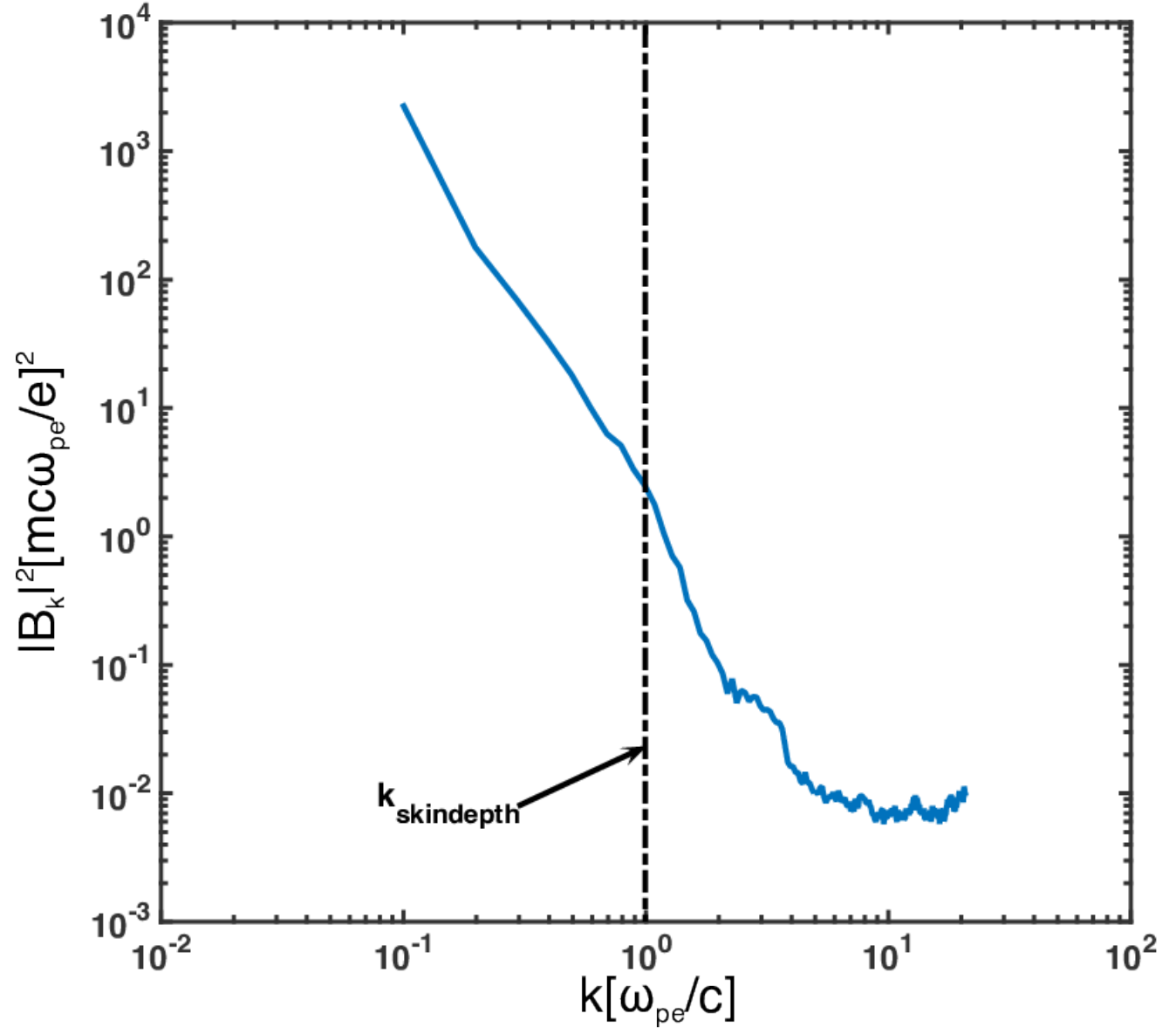


FIG. 6: Power spectrum of magnetic field spatial profile measured at pump-probe delay of 0.4 picoseconds